Towards gradient-based design optimization of fully-flexible tension-leg platform wind turbines

Towards gradient-based design optimization of fully-flexible tension-leg platform wind turbines

P Rohrer[1], E E Bachynski-Polić[1], and M Collette[2]

[1]Department of Marine Technology, Norwegian University of Science and Technology, Trondheim, Norway
[2] Naval Architecture & Marine Engineering Department, University of Michigan, Ann Arbor, USA

E-mail: peter.j.rohrer@ntnu.no

Abstract.
Novel technologies and design methods are needed to enable cost-competitive development of wind turbines with floating foundations. Tension-leg platforms have an established history in the oil and gas industry, though the complexity in coupled analysis of floating wind turbines generally has limited the exploration of novel concepts. The application of efficient, gradient-based optimization models has shown promise to overcome these difficulties and develop innovative designs. The core of this design optimization approach is an efficient coupled aero-hydro-servo-elastic dynamic model for a generic tension-leg platform wind turbine design, referred to as TLPOpt. The equation of motion is defined based on the generalized elastic mode shapes of the combined main column and tower. TLPOpt is implemented in the OpenMDAO framework for optimization, and analytical derivatives are defined throughout to increase efficiency. Stochastic dynamic analysis in the frequency-domain allows for efficient assessment of fatigue and extreme conditions. Verification steps show good agreement between the linearized analysis and higher-fidelity analysis tools. Early optimization studies suggest the optimization is able to improve upon a reference design, though more realistic constraint and objective functions are needed to draw further conclusions.

1. Introduction

Installations of offshore wind turbines have accelerated in recent years [1] as global interest in low-carbon energy has increased. Bottom-fixed offshore wind farms have proven popular in areas with large and relatively shallow continental shelves. In many densely populated regions water depth increases rapidly away from the coastline, necessitating floating foundations for offshore wind turbines. Several concepts for floating wind turbines have been introduced, borrowing from floating substructures developed for the offshore oil and gas industry [2]. Among these concepts are tension-leg platform wind turbines (TLPWTs) which rely on taut moorings to overcome 'excess' buoyancy of the hull. Tension-leg platforms typically experience nearly negligible motion in heave, roll, and pitch; and have a small seabed footprint as moorings are installed directly below the platform, providing an advantage where maritime space is shared with other industries. This work seeks to apply gradient-based design optimization methods to find innovative TLPWT designs.

Among the earliest attempts to use design optimization for offshore structures was a study by Clauss and Birk [3]. They optimized several base geometries, including a tension-leg platform, to reduce hydrodynamic loads with constraints on hydrostatic stability and geometry. Their findings suggest tendon loading is reduced by increasing distance between the tendon attachment points. Gradient-free optimization studies for floating wind turbine (FWTs) include works by Hall et al. [4] and Karimi et al. [5] Karimi et al. conducted a wider optimization of 5 MW floating wind turbine concepts considering single and multi-column substructures with tension and catenary moorings. The optimization sought to minimize platform cost and a performance metric for nacelle acceleration, and cost and performance constraints were also applied. The results indicated a tradeoff between nacelle acceleration and cost for each substructure, and generally semi-submersible designs were the least expensive for a given performance. These gradient-free approaches were generally limited to approximately ten design variables due to the computational cost of evaluating so many designs.

Gradient-based optimization methods make it possible to efficiently consider many more design variables by leveraging gradients to guide the optimization. Fylling and Berthelsen conducted an early gradient-based optimization of a spar-type FWT [6]. Their design included a simple parameterization with up to six design variables for a 5 MW spar-buoy with moorings and power cables included. They found the optimization was able to improve an unacceptable design, but had difficulties with inaccuracies in the approximated gradients. More recently, Hegseth [7] developed a linearized aero-hydro-servo-elastic model for a spar-type FWT with over 80 design variables that was shown to have good agreement with nonlinear time-domain simulations. The purpose for development of the linearized model was to enable gradient-based design optimization of the structure using analytical gradients. The SNOPT [8] optimization algorithm was used with the objective of minimizing cost of the FWT and variation in power output. The optimization model was also used to investigate alternative control strategies, environmental modeling, and fatigue safety factors. The present work expands upon Hegseth's work to apply gradient-based design optimization methods to a TLPWT design considering dozens of design variables.

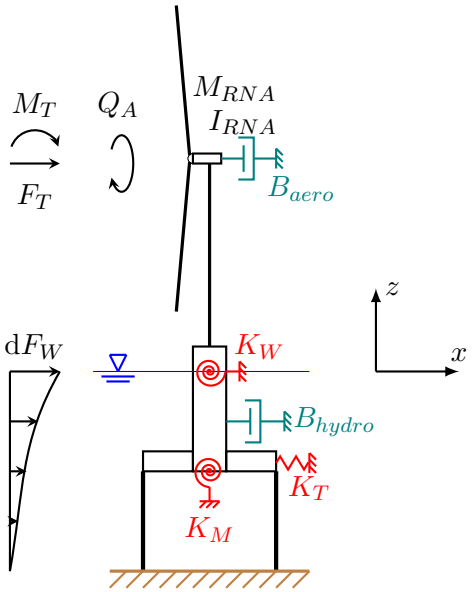

Figure 1: Linear dynamic model of the tension-leg platform wind turbine model in TLPOpt.

2. Model Development

The optimization model developed here, TLPOpt, is a linearized aero-hydro-servo-elastic model that describes the responses of a flexible TLPWT. In TLPOpt, the rotor design is fixed and outside the scope of the optimization. A sketch of the linearized model is shown in Figure 1. Wave forcing and viscous drag are applied to the submerged portion of the main column and pontoons. A thrust force and overturning moment from incoming wind act at the tower top, while an aerodynamic torque acts on the rotor. The rotor-nacelle assembly has a mass and moment of inertia. The rotor speed is defined by rotor inertia, generator torque, and aerodynamic torque. The model is agnostic to location, water depth, and the wind turbine generator used in the design. For the purposes of development, the DTU 10 MW reference turbine design [9] (hub height 119 m) in 200 m water depth is considered. The FWT substructure consists of a central circular column with structural scantlings, and horizontal pontoons modeled as rigid bodies. The substructure and tower are assumed to be made of steel, and concrete solid ballast is used in the central column if required. The TLPWT designs that TLPOpt considers are similar to 'SeaStar' tension-leg platform designs (see details in Leverette [10]), or the Glosten Pelastar™ design [11], though neither was used a reference for TLPOpt. A 10 MW TLPWT reference design from Tian's thesis [12] was used for the verification steps and as a starting point for optimization. The reference design did not consider fatigue damage and may not represent a truly feasible substructure design.

2.1. Hydrodynamic Loading

The hydrodynamic components of the model are based on two first-order wave load approximations, MacCamy-Fuchs's theory and the MOJS (Morison) equation. Analytical partial derivatives are defined to enable gradient-based optimization without the need for approximated derivatives. Wave loading on the main column of the hull is calculated using MacCamy-Fuchs's theory [13], which is based on an analytic solution of the diffraction problem for a vertical circular cylinder extending from the sea surface to the seabed. Wave loading on the pontoons is calculated using the MOJS equation [14], with both horizontal and vertical wave particle kinematics considered. Wave loading is calculated at specified wave frequencies, which are bounded to avoid very low frequencies and high frequencies where there is little wave excitation. No consideration is given to interaction between the column and pontoons, or end effects on any members. Higher-order wave loading can contribute significantly to the response of tension-leg platforms, however TLPOpt excludes higher-order wave loads. Constant added mass coefficients based on strip theory were applied following work by Bachynski [15]. The central column is assumed to be circular, while the pontoons can have circular or rectangular cross-sections using 2D coefficients from DNV GL [16]. End-effects and tangential added mass are neglected as they add significant complexity and comprise a small component of the total added mass.

2.2. Structural Dynamics

The design of larger floating support structures for future wind turbine generators requires more attention to be paid to structural dynamics. The wind turbine tower is typically the most flexible component of the structure due to its length and relatively lightweight design. Steel-efficient designs for large floating structures tend to behave elastically, and incorporating hull and tower flexibility has been shown by Borg et al. [17] to provide additional information on dynamic behavior of floating wind turbines. TLPOpt therefore considers the combined bending of the wind turbine tower and central column. The structural component of TLPOpt develops a finite element model of the column/tower using Euler-Bernoulli beam elements with four degrees of freedom per element. Each element is assigned a mass, geometric stiffness, and material stiffness based on the design variables. The rotor-nacelle assembly, the pontoons, and the tendons have

discrete, lumped contributions to the finite element model. Only bending in the surge-heave plane is considered, meaning all sway, heave, roll, and yaw motions are neglected. The primary function of developing the finite element model is to evaluate the free vibration of the structure by solving the eigenvalue problem. The resulting eigenvectors are used to analyze the structural response in the generalized modes of response using modal superposition, as detailed in Chapter 3 of Naess and Moan [18]. A sketch of the generalized modes found for the 10 MW reference design can be found in Figure 2.

2.3. Aerodynamic Loading

Many coupled models of floating wind turbines (such as OpenFAST from NREL [19]) use blade element/momentum (BEM) theory to compute loads on the turbine. In BEM theory, the blades are divided into elements radially from the hub to tip. Each element generates a lift and a drag force based on its angle of attack, which is a function of the rotor speed, wind speed, and induction factor. Traditionally, a number of additional corrections are applied to BEM theory; at a minimum the Prandtl correction for loss at the hub and tips and the Glauert correction for high induction factors [20]. In a quasi-steady approach such as TLPOpt, dynamic wake and stall effects are neglected. To accelerate computation, induction factors can be pre-computed and stored for wide ranges of blade pitches and tip-speed ratios. Because the final loads are the only result needed to interface with the coupled-model, a rotor effective speed (independent of changes in tower and substructure design) can be established to represent the wind-field with a scalar value. Rotor effective speeds are used to determine total frequency-dependent aerodynamic loads: F_T, M_T, Q_T. Aerodynamic damping is determined by the rotor aerodynamics (determined by the BEM solution embedded in the rotor effective speeds) and controller actions. A derivation of this approach is summarized in Appendix B of Hegseth's PhD thesis [7].

2.4. Control System

Baseline blade pitch and generator torque control systems are typically included in the design of reference turbines, while tuning of control parameters is done at a detailed design stage. The control system of TLPOpt is based on the NREL 5 MW reference turbine [21], with a simplified low-pass filter and no transition strategy. This controller uses generator torque control (with a single constant of proportionality) below rated wind speed and blade pitch control above rated wind speed. The blade-pitch control system parameters (proportional and integral gains) are variables in the optimization, allowing for future studies focused on control strategy variations.

2.5. Equation of Motion

A state-space model is used to represent the linear, time-invariant dynamic system that describes the floating wind turbine; closely following work by Hegseth [7]. This differs from traditional analyses of floating wind turbines, which have largely used nonlinear time-domain simulations. Carrying out these simulations at every iteration in the optimization would be computationally prohibitive. The state-space approach in TLPOpt combines two models, one for the structural or physical system, and another for the controls system, into a single closed loop linear system. To fully and fairly capture the advantages of flexible structures, in contrast to typical dynamic analysis of floating wind turbines, TLPOpt assumes no rigid modes of response. The structural response is assumed to be a combination of the first three elastic modes (which may include a combination of rigid body motions and bending) defined by the undamped structural model. The coefficient matrices and forcing vector are defined by these generalized modes, using the formulation from Chapter 3 in Naess and Moan [18].

$$\begin{aligned}\dot{\vec{x}}(t) &= \underline{\underline{A}}\vec{x}(t) + \underline{\underline{E}}\vec{u}(t)\\ \vec{y}(t) &= \underline{\underline{C}}\vec{x}(t) + \underline{\underline{D}}\vec{u}(t)\end{aligned} \tag{1}$$

$$\begin{aligned}\vec{x} &= \begin{bmatrix} x_1 & x_2 & x_3 & \dot{x_1} & \dot{x_2} & \dot{x_3} & \dot{\varphi} & \varphi_{lp} & \dot{\varphi}_{lp}\end{bmatrix}^T\\ \vec{u} &= \begin{bmatrix} v_{F_T} & v_{M_T} & v_{Q_A} & e^{i(\omega t)} & e^{i(\omega t)} & e^{i(\omega t)}\end{bmatrix}^T\end{aligned} \tag{2}$$

$$\underline{\underline{A}} = \begin{bmatrix} \underline{\underline{A_s}} & \underline{\underline{E_{sc}C_c}} \\ \underline{\underline{E_cC_s}} & \underline{\underline{A_c}}\end{bmatrix}, \quad \underline{\underline{E}} = \begin{bmatrix} \underline{\underline{E_{sd}}} \\ \underline{\underline{0}}\end{bmatrix}, \quad \vec{x} = \begin{bmatrix}\vec{x}_s \\ \vec{x}_c\end{bmatrix} \tag{3}$$

$$\underline{\underline{H}}(\omega) = \underline{\underline{C}}\Big(i\omega\underline{\underline{I}} - \underline{\underline{A}}^{-1}\Big)\underline{\underline{E}} + \underline{\underline{D}} \tag{4}$$

Each state-space model (and the closed loop system) can be written as a system of equations following the format of Equation (1). The state vector ($\vec{x}$) and inputs vector ($\vec{u}$) for the closed loop system are given in Equation (2). To create the closed-loop system, the outputs ($\vec{y}$) from the structural model are set equal to the inputs ($\vec{u}$) of the controls model, and the outputs from the controls model set equal to the controls inputs (not included in Equation (2)) for the structural model. The closed loop system state-space matrices can then be written as concatenations of the matrices from each model, shown in Equation (3), with submatrices defined below. The closed loop system is used to develop the generic transfer function (Equation (4)) for the linearized system based on the formulation from Chen [22]. A more detailed description of these models is given in Hegseth's PhD thesis [7].

The structural model follows from standard frequency-domain dynamic analysis, with the addition of a single degree of freedom rotor speed equation of motion. The model includes two states for each structural mode considered (x_1, x_2, x_3, $\dot{x}_1$, $\dot{x}_2$, $\dot{x}_3$), and one state for the rotor speed ($\dot{\varphi}$). The state matrix, $\underline{\underline{A_s}}$ is defined by classical inertia (including hydrodynamic added mass), damping, and stiffness matrices for frequency-domain analysis based on Chen [22]. There are two input matrices, one corresponding to external forcing, $\underline{\underline{E_{sd}}}$, and another corresponding to the control inputs $\underline{\underline{E_{sc}}}$. The output matrix, $\underline{\underline{C_s}}$ is a constant and sparse matrix that 'selects' the outputs (in this case, only the rotor speed) from the states. The feedthrough matrix, $\underline{\underline{D_s}}$ is a constant null matrix. The controls model is based on the baseline variable-speed blade-pitch controller described above. The model includes two states representing low-pass filtered rotor displacement and speed (φ_{lp}, $\dot{\varphi}_{lp}$). The state matrix ($\underline{\underline{A_c}}$) and input matrix ($\underline{\underline{B_c}}$) are developed to filter the rotor speed using a low-pass frequency (ω_{lp}). Two formulations of the output matrix ($\underline{\underline{C_c}}$) are used depending on if the mean wind speed is above or below rated wind speed, outputting either generator torque or blade pitch angle. The feedthrough matrix $\underline{\underline{D_c}}$ is again a constant null matrix.

3. Model Verification

Verification of the wave excitation and added mass in TLPOpt with results from WAMIT is presented in Figure 3. WAMIT [23] is a commercially available software for wave-structure interaction based on potential theory that can consider wave loading in generalized modes of deformation. There is agreement in the shape of wave excitation magnitude and phase between the linear potential solution from WAMIT and TLPOpt. The difference in the magnitude of the peak of the excitation is less than 10% for both mode 1 and mode 2. Mode 3, the modeshape

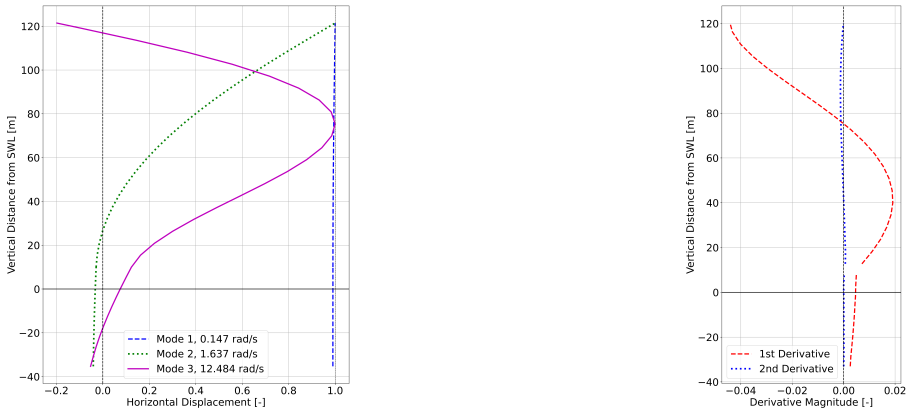

(a) First three generalized modeshapes.

(b) First and second derivative of generalized third modeshape.

Figure 2: Generalized modeshapes of 10 MW TLPWT reference design from TLPOpt.

with the most curvature (see plots in Figure 2), shows the largest discrepancy (up to 27.5% of maximum) in excitation from TLPOpt. WAMIT also provides frequency-dependent added mass coefficients, and in Mode 1 and Mode 2 the constant value estimate from TLPOpt is of the same order of magnitude. In mode 1, the frequency-dependent value is within 35% of the constant value, while in mode 2 the frequency-dependent value is within 25% of the constant value. The constant added mass estimate in Mode 3 is up to three times larger than the WAMIT results at some frequencies. This is believed to be due to the lack of element rotation in the generalized modes in WAMIT. Specifically, WAMIT considers only horizontal displacement of panels in forming modeshapes, while TLPOpt includes rotation in addition. The rotation is significant in Mode 3, such that the WAMIT results are not a perfect benchmark.

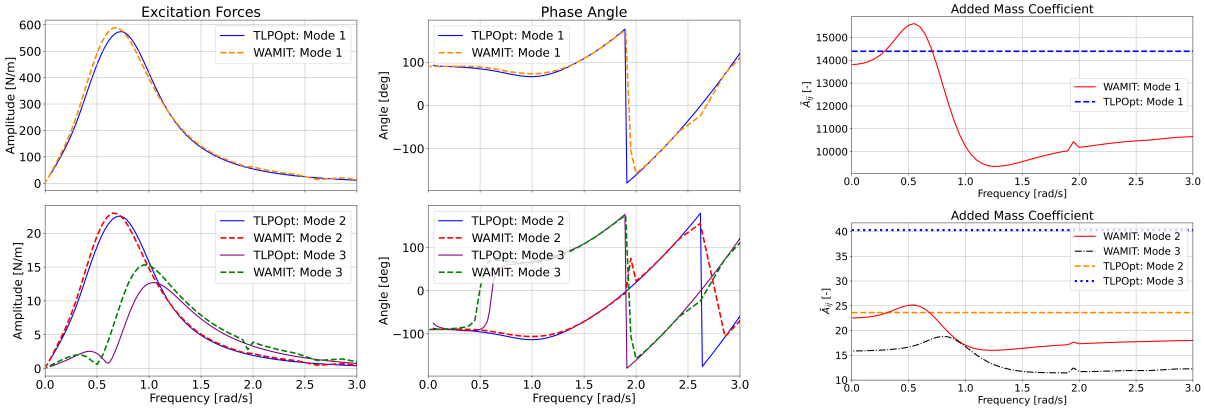

Figure 3: Frequency-domain forcing and added mass from TLPOpt and WAMIT.

Verification of the rotor thrust force, aerodynamic torque, and rotor speed in TLPOpt is presented in Figure 4. The aerodynamic loading based on rotor effective speeds in TLPOpt is compared to dynamic BEM results from nonlinear aero-hydro-servo-elastic time domain analysis in SIMA (an analysis tool developed by SINTEF Ocean [24, 25]) using a turbulent wind input

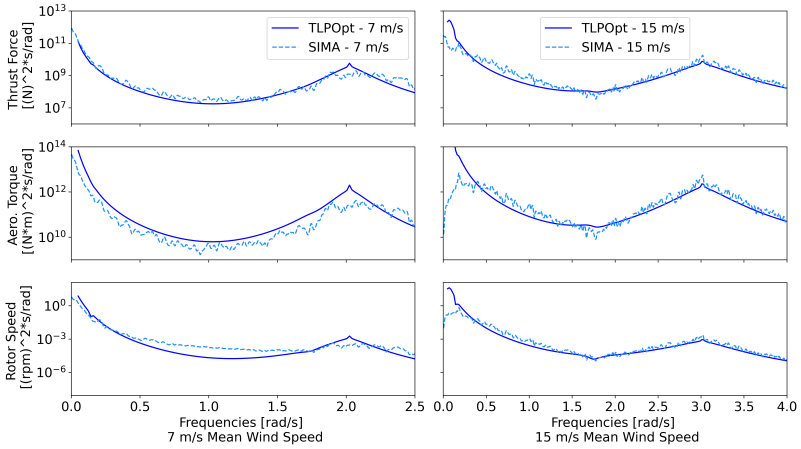

Figure 4: Aerodynamic loads at tower top and rotor speed from SIMA model with turbulent wind field, and TLPOpt analysis with identical conditions.

and no waves. The results show agreement qualitatively similar to results from Hegseth [7] with a mean wind speed of $15\,\mathrm{m\,s^{-1}}$ (above turbine rated speed), with the exception of very low frequencies. The agreement is poorer with a mean wind speed of $7\,\mathrm{m\,s^{-1}}$ (below turbine rated speed), due to slight differences in the controller used in TLPOpt and SIMA.

The response of the model to wave excitation is verified against SIMA in Figure 5. Verification against another software tool introduces additional uncertainties, though it is unavoidable given the current lack of benchmark experimental results for TLPWTs. There is a need for additional experimental results for future verification of novel analysis models. The TLPWT is modeled in SIMA with a combination of rigid bodies (for the RNA and pontoons) and a finite element model for the column and tower, with the same structural properties as the finite element model in TLPOpt. Time-domain simulations are run and post-processed to compare with frequency-domain responses from TLPOpt. The verification presented in Figure 5 shows agreement in shape in magnitude of the response spectra, though TLPOpt seems to underpredict response at the peak wave-frequency (see Figure 5b) and overpredict the resonant response. It is not clear whether this is a persistent issue in the analysis model, or a unique issue with the reference design considered.

4. Optimization Problem

A wide range of potential optimization problems could be developed using the TLPOpt model. In this work, the objective of the optimization is to minimize standard deviation of acceleration at the nacelle. The design variables describe the structure of the hull, moorings, and tower. Constraints are applied to exclude designs that are physically infeasible, designs that are likely to fail due to extreme conditions, and designs that exceed a cost limit. The current model is limited to assess dynamic response in a single environmental condition, and excludes dynamic tendon response and fatigue damage constraints. An objective of minimizing nacelle accelerations was chosen to demonstrate the ability of TLPOpt to consider wave loading and response, as the constraints are primarily related to wind loading and response.

4.1. Design Variables

In the simplified model, the design variables describe the geometry of the substructure only, and the tower design is held constant. The design variables are vectorized with a fixed number

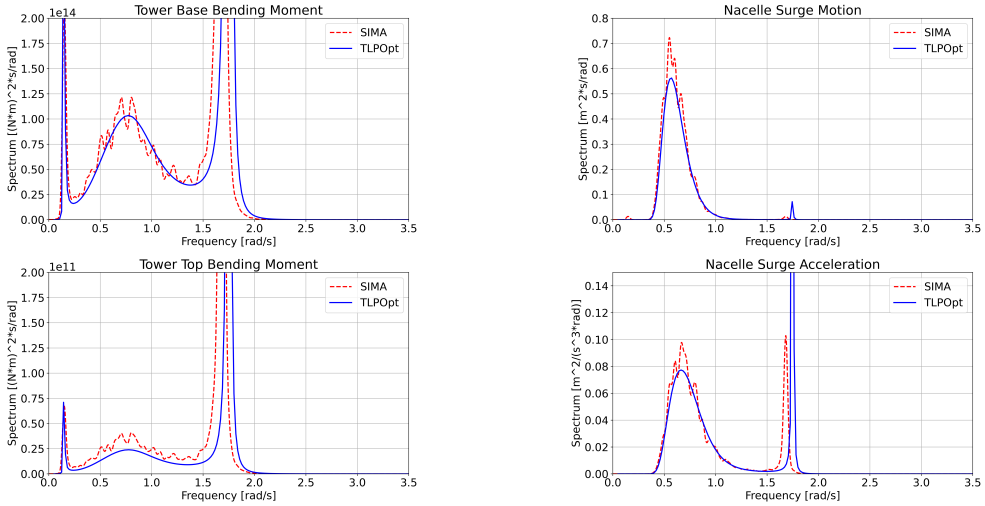

(a) Tower base and top bending moment due to white noise spectrum.

(b) Nacelle motion and acceleration due to moderate ($H_s = 2.5\,\mathrm{m}$) JONSWAP spectrum.

Figure 5: Tower and nacelle response to wave excitation from TLPOpt and SIMA.

of segments along the central column. The shape and number of pontoons is a parameter that is fixed throughout the optimization, however pontoon sizing is varied. The tendon outer diameter is a design variable, while the inner diameter is a result of requiring the tendon to be neutrally buoyant. Finally, a ballast factor is included to allow for permanent ballast in the main column to aid in stability. There are a total of 36 design variables, outlined in Table 1.

Table 1: Design variables implemented in the current model.

Variable	Units	Meaning
D_c	[m]	Vector (11 x 1) of outer diameters of main column segments at ends.
L_c	[m]	Vector (10 x 1) of lengths (measured vertically) of main column segments.
t_c	[m]	Vector (11 x 1) of wall thicknesses of main column segments at ends.
L_p	[m]	Length of pontoons, measured from edge of main column to pontoon tip.
D_p	[m]	Outer diameter or side length of pontoons.
D_t	[m]	Outer diameter of tendons.
BF	[-]	Ballast weight added as a fraction of main column displacement.

4.2. Constraints

Constraint functions define the feasibility of a design, and prevent the optimizer from reaching impossible solutions. The constraint functions should not include any preconceived notions of what the optimal design might look like to afford the optimizer maximum flexibility. The current version of TLPOpt applies simplified response constraints. To avoid tendon failure, tendons are constrained to avoid negative tension and stress exceeding yield with the maximum thrust force applied. Because dynamic tension variation is not considered, a minimum of 1000 kN of tension is required in the lowest tension tendon, and a maximum stress of 125 MPa is allowed in the highest tension tendon. To avoid excessive loading on tendon connections, the maximum static surge offset (based only on thrust force) is limited to 5% of the water depth, and static pitch angle is limited to 0.5 degrees. The diameter of hull segments is constrained to avoid abrupt

changes and ensure manufacturability by limiting the taper angle of each segment. Finally to prevent the optimizer from making the design less cost-efficient than the reference design, a constraint is added to the cost function. The maximum value of the cost constraint is based on the output of the cost function for the reference design from Tian [12], though the cost function used has not been extensively verified.

4.3. OpenMDAO Implementation

The optimization model is implemented in OpenMDAO [26], an open-source framework for multidisciplinary design optimization. The multidisciplinary analysis model (MDA) described above is written in pure Python (using the Numpy and Scipy packages) and is structured to interface with the framework of OpenMDAO. Each component in the model includes analytical definitions of its partial derivatives. OpenMDAO exploits state-of-the-art methods for efficiently calculating total derivatives and makes use of the overall sparsity of the problem. The SNOPT [8] optimization algorithm was used to drive the optimization.

Table 2: Selected characteristics of initial and 'optimal' designs from two wave conditions.

Variable	**Reference Design**	**Mild Wave**	**Extreme Wave**
Std. Dev. Nacelle Accel. [$\mathrm{m\,s^{-2}}$]	0.217 (mild) 0.506 (ext.)	0.167	0.357
Tendon Pretension [kN]	29360	18500	15600
Mean Surge Offset [m]	2.13	3.10	3.67
Mean Pitch Angle [deg]	0.003	0.007	0.008
Mode 1 Natural Period [s]	42.5	59.7	64.2
Mode 2 Natural Period [s]	3.56	3.80	3.76
Hull Volume [$\mathrm{m^3}$]	17310	19880	18730
Substructure Mass [t]	7314	13280	12980
Ballast Mass [t]	4456	10000	9781
Column Draft [m]	35.3	49.5	49.3

4.4. Preliminary Results

Optimization runs were attempted using the simplified model and show promising results despite the limitations of considering only one environmental condition. Selected parameters of the optimal designs and reference design are presented in Table 2. Two runs were conducted, a mild wave ($H_s = 2.5\,\mathrm{m}$, $T_p = 10.2\,\mathrm{s}$) and an extreme wave ($H_s = 7.5\,\mathrm{m}$, $T_p = 12\,\mathrm{s}$) condition, both with mean wind speed at the turbine's rated speed ($11.4\,\mathrm{m\,s^{-1}}$). Rated wind speed was chosen to maximize thrust force, and nonlinear effects of control strategy 'switching' at rated speed are not seen due to the lack of control transition region. Each optimization run took approximately 30 minutes to complete on a standard workstation computer. While it is not possible to draw broad conclusions about TLPWT design from these limited optimizations, the difference in wave environment appears to affect the 'optimal' design. Both optima reduce the standard deviation of nacelle acceleration. This is possible by increasing main column volume and ballast weight, while decreasing tendon diameter. As a result pretension decreases significantly, and the natural periods and mean static offset increase. The difference between the two optimal designs is small, likely due to the limited impact of wave loading and response on the current optimization problem. Furthermore, because cost was not the objective of this optimization, these designs are likely inefficient with material usage and 'overbuilt' for the environmental conditions considered. Further work can address these shortcomings with different selections of objective and constraint functions, and further refinement of the analysis model.

5. Conclusions

The model and results presented show that gradient-based optimization can be used to efficiently assess tension-leg platform wind turbine designs. TLPOpt combines an efficient analysis model and analytically-defined partial derivatives to enable optimization with dozens of design variables. The resulting optimal designs show significant cost reduction using simplified cost models and constraints. Future work will expand upon these results, implementing more realistic constraints on dynamic response and fatigue life.

Acknowledgments

This work has been funded by the Research Council of Norway, through SFI BLUES, grant number 309281. Portions of the model were constructed during Master's thesis research, supported by the U.S.-Norway Fulbright Foundation.

References

[1] WindEurope 2021 Offshore wind in Europe – key trends and statistics 2020 Tech. rep. WindEurope
[2] Twidell J and Gaudiosi G (eds) 2009 *Offshore Wind Power* (Multi-Science Pub. Co) ISBN 978-0-906522-63-9
[3] Clauss G F and Birk L 1998 *Applied Ocean Research* **18** 157–171
[4] Hall M, Buckham B and Crawford C 2013 *2013 MTS/IEEE OCEANS - Bergen* pp 1–10
[5] Karimi M, Hall M, Buckham B and Crawford C 2017 *Journal of Ocean Engineering and Marine Energy* **3** 69–87
[6] Fylling I and Berthelsen P A 2011 *ASME 2011 30th International Conference on Ocean, Offshore and Arctic Engineering* pp 767–776
[7] Hegseth J M 2020 *Efficient Modelling and Design Optimization of Large Floating Wind Turbines* Ph.D. thesis Norwegian University of Science and Technology
[8] Gill P E, Murray W and Saunders M A 2005 *SIAM Review* **47** 99–131
[9] Bak C, Zahle F, Bitsche R, Kim T, Yde A, Henriksen L, Andersen P B, Natarajan A and Hansen M H 2013 *Wind Energy* **124**
[10] Leverette S J and Hodges S B 2020 (*Offshore Technology Conference* no OTC-30752-MS)
[11] Hurley W L and Nordstrom C J 2014 PelaStar Cost of Energy: A cost study of the PelaStar floating foundation system in UK waters FEED Study 12004.1 Glosten
[12] Tian X 2016 *Design, Numerical Modelling and Analysis of TLP Floater Supporting the DTU 10MW Wind Turbine* Master's Norwegian University of Science and Technology
[13] MacCamy R and Fuchs R A 1954 Wave forces on piles: A diffraction theory Technical Memorandum 69 Beach Erosion Board, Corps of Engineers
[14] Morison J, Johnson J and Schaaf S 1950 *Journal of Petroleum Technology* **2** 149–154
[15] Bachynski E E 2014 *Design and Dynamic Analysis of Tension Leg Platform Wind Turbines* Ph.D. thesis Norwegian University of Science and Technology
[16] DNV GL 2011 DNV-RP-H103: modelling and Analysis of Marine Operations Recommended Practice DNV-RP-H103 DNV GL
[17] Borg M, Hansen A M and Bredmose H 2016 *Journal of Physics: Conference Series* **753** 082024
[18] Naess A and Moan T 2013 *Stochastic Dynamics of Marine Structures* (Cambridge University Press) ISBN 978-0-521-88155-5
[19] openFAST *OpenFAST Documentation — OpenFAST v2.5.0 Documentation* NREL
[20] Burton T (ed) 2011 *Wind Energy Handbook* 2nd ed (Wiley) ISBN 9780470699751
[21] Jonkman J, Butterfield S, Musial W and Scott G 2009 Definition of a 5-MW Reference Wind Turbine for Offshore System Development Tech. Rep. NREL/TP-500-38060 National Renewable Energy Lab. (NREL), Golden, CO (United States)
[22] Chen C T 2013 *Linear System Theory and Design* fourth edition ed The Oxford Series in Electrical and Computer Engineering (Oxford University Press) ISBN 978-0-19-995957-0
[23] Lee C H and Newman J 2005 *Computation of wave efects using the panel method* vol 1 (WIT Press) p 211–251 1st ed ISBN 9781853128370
[24] SINTEF Ocean *SIMO User Guide*
[25] SINTEF Ocean *RIFLEX User Guide*
[26] Gray J S, Hwang J T, Martins J R R A, Moore K T and Naylor B A 2019 *Structural and Multidisciplinary Optimization* **59** 1075–1104